

# Applying of EBIV technique for investigation of electrophysical parameters of devices based on HTSC

© S.V. Baryshev<sup>¶</sup>, A.V. Bobyl, O.P. Kostyleva

Ioffe Physicotechnical Institute, Russian Academy of Sciences,  
194021 St. Petersburg, Russia

(Получена 22 сентября 2006 г. Принята к печати 3 октября 2006 г.)

The local investigations with  $4\mu\text{m}$  spatial resolution using EBIV-signal registration of YBCO microstripes were made with low-temperature scanning microscopy technique. These investigations coupled with microwave measurements of YBCO films (near-field microscopy) and structural investigations (X-ray diffractometry, SEM) gave the correlation between half-widths of temperature dependence of third harmonic power maximum  $W_{\text{TH}}$ , EBIV-signal curve  $W_{\text{EBIV}}$  and average microcrystallite size. In order to explain such dependence diphasic medium model considering non-linear voltage-current characteristic of superconductor was proposed. Calculations allow us to conclude, that triple increase of microcrystallite size results in hundredfold reduction of non-linearity coefficient of YBCO films and microwave devices based on these films.

PACS: 74.25.Nf, 74.70.Ad, 74.72.Bk

## 1. Introduction

To begin with, according to recent data high temperature oxide superconductors (HTSC) can be regarded as some kind of semiconductor with especial type of energy-band structure [1,2]. Also the techniques based on affecting the electrophysical parameters of semiconductor devices such as EBIC and EBIV-techniques are far-famed. For example, these procedures allow one to determine widths of  $p$ - $n$ -junctions, various kinds of relaxation time parameters of structures and devices based on Si or A<sup>III</sup>B<sup>IV</sup> group materials. Also it's available to determine spatial fluctuations of the locally available open circuit voltage  $V_{\text{oc}}$  with significant consequences for the overall conversion efficiency of different photovoltaic devices. In particular, EBIV-method possesses useful advantage, i. e. it enables to visualize spatial distribution map of sample inhomogeneities by means of induced voltage mode.

Investigations to be given in the present paper deal with  $\text{YBa}_2\text{Cu}_3\text{O}_{7-x}$  structural quality affecting the non-linear microwave (MW) features and electrophysical parameters of the films and devices based on these films as consequence. The correlation between average microcrystallite size and half-widths of the third harmonic signal maximum and EBIV-signal is determined. In order to understand experimental results the diphasic model considering nonlinear current-voltage characteristic of superconductor was suggested. Calculations let us conclude, that triple increase of microcrystallite size results in hundredfold reduction of non-linearity coefficient of YBCO films and microwave devices based on these films. In a little while the necessity of EBIV-technique application in MW investigations of HTSC will be shown.

## 2. Samples. Experimental methods

Epitaxial  $\text{YBa}_2\text{Cu}_3\text{O}_{7-x}$  films of  $d = 0.7$ – $0.9\mu\text{m}$  thickness were fabricated from targets of (1:2:3) and (2:3:5) stoichiometric compositions with magnetron sputtering technique. The films were grown on  $\text{LaAlO}_3$  substrates in  $\text{Ar}/\text{O}_2$  gases mixture under 40 Pa pressure and at  $750^\circ\text{C}$  substrate temperature [3]. A set of 10 films of similar technological growth parameters, thicknesses and most structure perfection (surface morphology, X-ray reflex widths) was chosen. The temperature of superconducting transition was in 86–92 K range and transition width — 0.2–3.6 K.

We used the following parameters as criteria for structural perfection:  $c$ -axis parameter, lattice deformation along  $c$ -axis,  $\varepsilon = (c - c_0)/c = \delta c/c$ , where  $c_0 = 11.66 \text{ \AA}$  — lattice constant of bulk  $\text{YBa}_2\text{Cu}_3\text{O}_7$  monocrystal and microdeformation (dispersion of  $\varepsilon$ )  $\delta\varepsilon = \{(\delta c/c)^2\}^{1/2}$ . The coherent scattering area (average microcrystallite size)  $a$  [4] was defined along  $c$ -axis with the help of X-ray reflex half-width  $w_{\theta-2\theta}$  dependence on Bragg's angle in  $\theta$ - $2\theta$  scanning mode:

$$w_{\theta-2\theta} = w_\varepsilon^2 + w_a^2 = (2 \cdot \delta\varepsilon \cdot \text{tg } \theta_b)^2 + \left( \frac{\lambda_{\text{Cu}}}{2 \cdot a \cdot \cos \theta_b} \right)^2. \quad (1)$$

For this reason diffraction curves were registered by Rigaku ( $D_{\text{max}} - B/RC$ ) diffractometer with a special collimation scheme which reduces initial beam widening ( $\lambda_{\text{Cu}} = 1.54183 \text{ \AA}$ ).

Two independent experimental techniques were used to search correlations between structural and electrophysical parameters: 1) near-field MW (microwave) technique with spatial resolution as large as  $50\mu\text{m}$ ; 2) the technique based on EBIV-signal registration for investigation of YBCO microstripes with  $4\mu\text{m}$  spatial resolution. Investigations of electrophysical parameters and non-linear response were made with foregoing microscopy methods.

<sup>¶</sup> E-mail: lolapalooza@mail.ru

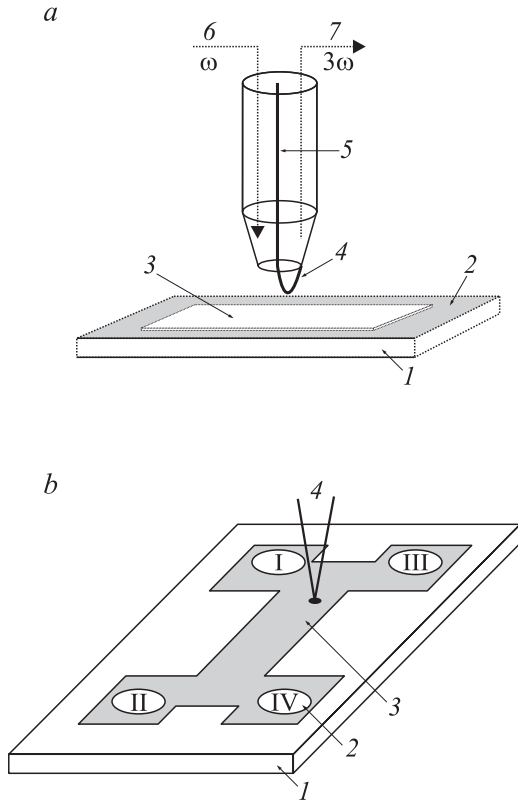


**Figure 1.** a) Scheme of near-field MW technique: 1 — LaAlO<sub>3</sub> substrate, 2 — YBa<sub>2</sub>Cu<sub>3</sub>O<sub>7-x</sub> film, 3 — teflon protective film, 4 — near-field MW probe, 5 — coaxial cable, 6 — incident MW signal, 7 — reflected MW signal. b) EBIV technique scheme: 1 — LaAlO<sub>3</sub> substrate, 2 — Ag contact, 3 — superconducting YBa<sub>2</sub>Cu<sub>3</sub>O<sub>7-x</sub> stripe, 4 — electron probe. I-IV — four-contact configuration for parasite contact resistance compensation.

For local investigation of non-linear MW response near-field non-linear MW technique was used. Under incident irradiation ( $\omega = 472$  MHz, see Fig. 1, a) higher harmonics are generated due to non-linear properties of HTSC films. All these harmonics are registered with inductive type probe; and then we were able to extract third harmonic signal (signal on  $3\omega = 1.4$  GHz frequency) using band-pass filter circuit. For additional details see Ref. [5].

The second procedure based on electron beam induced voltage registration (low-temperature scanning microscopy) is shown in Fig. 1, b. Originally, this technique was created and developed for conventional superconductor investigations [6] and also to study critical temperature spatial distribution in HTSC films [7]. Electron beam heats some local area of SC microstripe, as consequence, such heating results in local resistance changes and the voltage magnitude registered. This electron beam induced voltage, EBIV-signal, is proportional to temperature derivative  $\frac{\partial \rho(r, T, j)}{\partial T}$  of local resistance of given the stripe area  $\rho$ . Signal maximum is in temperature axis point where highest steepness of  $\rho(T)$  dependence exists. This point can be interpreted as a critical temperature of local superconducting transition,  $T_c$ . The

half-width of the curve maximum corresponds to the width of superconducting transition  $\Delta T_c$ . Electron beam scanning, we were able to determine spatial distributions of  $T_c$  and  $\Delta T_c$  ( $T_c$  and  $\Delta T_c$ -mapping) with  $4 \mu\text{m}$  spatial resolution and with 0.1 K temperature precision. Measurements of EBIV-signals were carried out with CamScan Series 4-88 DV 100 electron microscope provided nitrogen cooling system, thermo-controller ITC 4 and intrachamber preamplifier were used to decrease noise intensity. Temperature could vary within the range from 77 to 300 K with 0.1 K step (i.e. with corresponding precision). Bias voltage changed from 0.2 to 0.7 V at 2–7 mA current variations. These regimes provided the ability of EBIV-signal magnitude measurements (that is to say, such experimental conditions allowed one to get steady and reasonable signal values) and didn't bring any distorts in signal value. To increase signal-noise ratio synchronously-selective method was used at 20 kHz frequency. Beam current was about  $10^{-8}$  A at 15 kV accelerating voltage.

Fig. 2 represents simple general scheme of all signals and parameters used in the present paper: temperature dependences of MW signal power at third harmonic frequency, EBIV-signal curve, temperature dependence of specific resistance  $\rho(T)$  and critical current  $j_c(T)$ . As is well known, the temperature dependence of third harmonic (TH) power demonstrates its peak nearby the critical temperature [8,9], and non-linear response arises at temperatures below current percolation threshold temperature —  $T_{pr}$ . Under such temperatures, a half of film bulk is enough to be superconductive for specific resistance  $\rho(T)$  becoming zero; in this situation contact technique (EBIV) is useless. At the same time local EBIV-signal measurement is possible in temperature region where resistance is nonzero, i.e. at temperatures above  $T_{pr}$ .

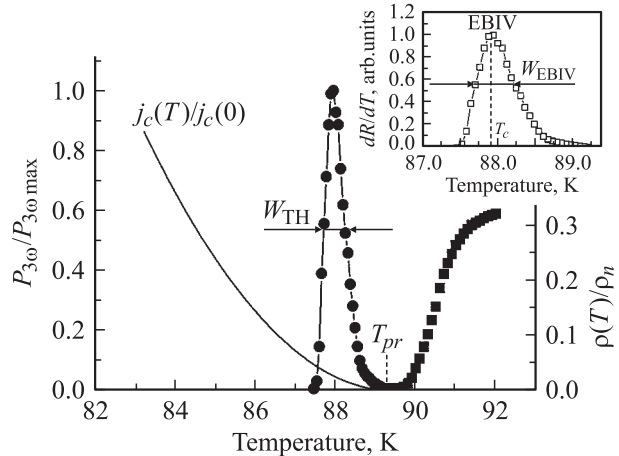


**Figure 2.** Temperature dependences of third harmonic power  $P_{3\omega}(T)$ , microstripe resistance  $\rho(T)$  normalized to normal phase resistance (at  $T = 300$  K) and temperature dependence of effective critical current  $j_c(T)$  for YBa<sub>2</sub>Cu<sub>3</sub>O<sub>7-x</sub> film. The inset represents temperature dependence of EBIV-signal curve (for different film). The figure shows also percolation temperature —  $T_{pr}$  and critical temperature of SC transition  $T_c$  in EBIV technique.

Thus, signal registration regions of both techniques being situated in different temperature ranges, their combination can give complementary information about superconducting properties nearby transition temperature to normal state (nearby the percolation threshold). Also the higher resolution of LTSEM allows one to relate MW properties with the structure of superconductors more thoroughly.

### 3. Experimental results: correlation of SC and structural parameters. Theoretical model and calculation results

Fig. 3 shows the half-width dependence of TH (solid circles) and EBIV (solid squares) signals on average microcrystallite size. It can be easily seen that half-width of the signals obtained by two independent techniques increases as the crystallite size reduces.

The TH signal half-widths were determined as follows. Temperature dependencies of the signal at third harmonic frequency were recorded from an area as large as  $50 \times 1000 \mu\text{m}^2$  — the area of MW probe. Then the half-width of the signal for each sample was measured and the dependence of  $P_{3\omega}$  function half-width on average microcrystallite size  $W_{\text{TH}}(a)$  was built up (Fig. 3,  $a$ , solid circles). Since lateral resolution of non-linear near-field MW microscopy is as large as  $50 \times 1000 \mu\text{m}^2$ , this technique is an integral method over a large assembly of crystallites in SC films. On account of low resolution of near-field microscopy low-temperature scanning microscopy (LTSEM) was used for investigation of non-linear peak widening mechanism in vicinity of  $T_c$  and to receive detailed information about microstructure affecting MW properties.

In LTSEM case the half-width determination procedure was more complicated, since temperature dependencies of integral resistance and resistances of local areas can differ frequently. This procedure allows to obtain a  $T_c$ -maps [10] and plot distribution functions of film fragments on critical temperature —  $F(T_c)$ , while using the possibility of local EBIV-signal registration can give temperature dependence of local resistance  $\rho_i(T)$  obtained from EBIV-signal curve of fragment  $f(T_{ci}, T)$ . If one describes  $T_c$  non-uniformity with the help of distribution functions, it's important to make a proposition of statistical independence of fragments and crystallites on critical temperature based on inequality (effective medium approach):  $\xi \ll a \ll r \ll L$ , where  $\xi$  — coherence length (2–10 Å);  $a$  — average crystallite size (0.2–0.8  $\mu\text{m}$ );  $r$  — average fragment size (4–5  $\mu\text{m}$ );  $L$  — microstripe dimension (100–600  $\mu\text{m}$ ). Further, in order to avoid faults an additional procedure of experimental results treatment was used, since temperature dependencies of integral resistance and resistances of local areas can differ. Namely, convolution procedure for  $F(T_c)$  and  $f(T_{ci}, T)$  functions was produced. Firstly, the curve of local specific resistance of fragments  $\rho_i(T_{ci}, T)$  must be found by means

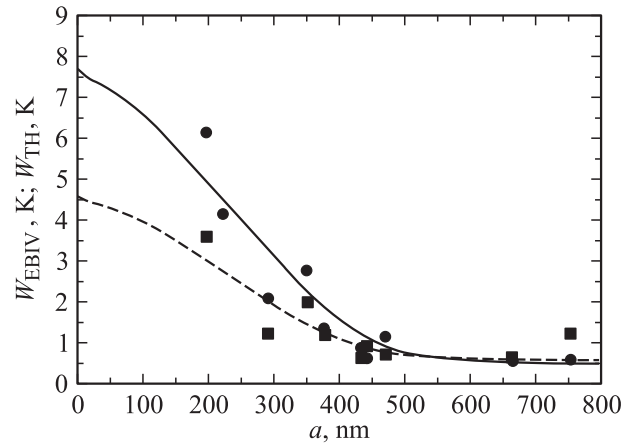


**Figure 3.** Half-width of third harmonic signal peak (solid circles)  $W_{\text{TH}}$  and EBIV-signal half-width  $W_{\text{EBIV}}$  (solid squares) dependence on average microcrystallite size  $a$  for  $\text{YBa}_2\text{Cu}_3\text{O}_{7-x}$ . Solid and dash lines are approximation of  $W(a)$  based on effective medium model for non-linear response and EBIV-signal, respectively.

of EBIV-signal:

$$\rho_i(T_{ci}, T) = \int_0^T \frac{f(T_{ci}, T)W}{j \cdot \Delta T \cdot \Lambda^2} dT, \quad (2)$$

where  $j(r, T)$  — local current density,  $\Lambda$  — characteristic temperature field size,  $W$  — microstripe width,  $\Delta T$  — temperature of local heating. Then specific resistance of effective medium for two-dimensional case  $\langle \rho \rangle(T)$  [10–12] must be determined at MW probe scale:

$$\sum_{i=1}^n \frac{\langle \rho \rangle(T) - \rho_i(T_{ci}, T)}{\langle \rho \rangle(T) + \rho_i(T_{ci}, T)} F(T_{ci}) = 0. \quad (3)$$

Further one can find restored function  $S_{\text{EBIV}}(T)$  at MW probe scale:

$$S_{\text{EBIV}}(T) = \frac{I_s}{W} \cdot \frac{\partial \langle \rho \rangle(T)}{\partial T} \Delta T, \quad (4)$$

where  $I_s$  — current strength at  $50 \mu\text{m}$  scale. As a result we have restored temperature dependence of local EBIV-signal at MW probe scale ( $50 \mu\text{m}$ ) —  $S_{\text{EBIV}}(T)$ . These  $S_{\text{EBIV}}(T)$  half-widths are marked in Fig. 3 as  $W_{\text{EBIV}}(a)$  (solid squares).

For interpretation of experimental result shown in Fig. 3 let's briefly formulate the phenomenological model of diphasic superconductor: superconducting film consists of the first phase in the form of cylindrical superconducting crystallites (grains) placed into the second medium called matrix (the second phase). To put it in another way, the first phase models superconducting properties of microcrystallite, while another one describes the presence of intergranular space in SC films.

Model  $E(j, T)$  dependence of these media considered to be current-voltage characteristic of a single anhysteretic josephson junction [13] due to its typical features presented

in all models of resistive state. Besides, such a current-voltage characteristic describes main MW and transport properties of superconductors in vicinity of  $T_c$  and gives the relation of current with electric field in wide temperature range. The relations between electric field strengths  $E_1$ ,  $E_2$  and critical current densities of first medium  $j_1$  and the second one  $j_2$  are:

$$E_1(j_1, T) = \rho_{n1} \text{sign}(j_1) \sqrt{j_i^2 - j_{c1}^2(T)} \frac{j_1}{j_1}, \quad (5)$$

$$E_2(j_1, T) = \rho_{n1} \text{sign}(j_1) \sqrt{j_i^2 - j_{c1}^2(T)} \frac{j_2}{j_1}, \quad (6)$$

where  $j_{c1}(T)$  and  $j_{c2}(T)$ ;  $\rho_{n1}$  and  $\rho_{n2}$  — critical current densities and specific resistances of these phases, respectively. Here superconductivity parameters,  $j_c, \rho_n$ , are accepted as different in different phases ( $j_{c1}$  is proposed to be larger than  $j_{c2}$  and  $\rho_{n1} < \rho_{n2}$ ).

So, we use additional theses of our phenomenological model in the following mathematical form (Maxwell–Garnett approach):

$$E_1 = \frac{2\sigma_2}{\sigma_1 + \sigma_2} E_2, \quad (7)$$

where  $\sigma_1$  and  $\sigma_2$  are conductivities of the first and the second phases, respectively. Using effective model approximation:

$$p \frac{\langle \rho \rangle - \rho_1(j_1, T)}{\langle \rho \rangle + \rho_1(j_1, T)} + (1 - p) \frac{\langle \rho \rangle - \rho_2(j_2, T)}{\langle \rho \rangle + \rho_2(j_2, T)} = 0, \quad (8)$$

where  $\langle \rho \rangle = \langle E \rangle / \langle j \rangle$  — effective specific resistance,  $\rho_1 = E_1(j_1, T) / j_1$ ,  $\rho_2 = E_2(j_2, T) / j_2$  — effective specific resistances of the first and the second phases, and taking into account that  $\langle j \rangle = p \cdot j_1 + (1 - p)j_2$  [14] and  $\langle E \rangle = p \cdot E_1(j_1, T) + (1 - p)E_2(j_2, T)$ , we can get approximation of experimental curves (see Fig. 3, solid and dash lines).

#### 4. Conclusion

The local investigations using EBIV-signal registration of YBCO microstrips with  $4\mu\text{m}$  spatial resolution were made with low-temperature scanning microscopy (LTSEM) technique. These investigations coupled with microwave measurements of YBCO films (near-field microscopy) and structural investigations (X-ray diffractometry, SEM) gave the correlation between half-widths of temperature dependence of third harmonic power maximum  $W_{TH}$ , EBIV-signal curve  $W_{EBIV}$  and average microcrystallite size. In order to explain such dependence a diphasic medium model considering non-linear current-voltage characteristic of superconductor was proposed. Calculations allow to conclude, that triple increase of microcrystallite size results in hundredfold reduction of non-linearity coefficient of YBCO films and microwave devices based on these films.

#### References

- [1] V.E. Gasumiants, V.I. Kaidanov, E.V. Vladimirskaya. *Physica C*, **248**, 255 (1995).
- [2] K.V. Mitsen, O.M. Ivanenko. *JETP*, **79**, 1469 (2000).
- [3] A.A. Melkov, Y.-J. Oh, S.F. Karmanenko, D.A. Nikolaev, S.V. Baryshev. *IEEE Int. Students Seminar on MW applications of Novel Physical Phenomena (St.Petersburg Electrotechnical University, St.Petersburg, 2002)*. P. 13.
- [4] A.V. Bobyl, M.E. Gaevskii, S.F. Karmanenko, R.N. Kutt, R.A. Suris. *J. Appl. Phys.*, **82** (3), 1274 (1997).
- [5] A.A. Андронов, Е.Е. Пестов, Ю.Н. Ноздрин, В.В. Курин, А.Ю. Аладышкин, А.М. Куколо, Р. Монако, М. Боффа. *Изв. вузов. Радиофизика*, **46** (2), 123 (2003).
- [6] J.R. Clem, R.P. Huebener. *J. Appl. Phys.*, **51**, 2764 (1980).
- [7] M.E. Gaevski, A.V. Bobyl, S.G. Konnikov, D.V. Shantsev, V.A. Solov'ev, R.A. Suris. *Scanning Microsc.*, **10**, 679 (1996).
- [8] I. Ciccarello, C. Fazio, M. Guccione, M. Li Vigni, M.R. Trunin. *Phys. Rev. B*, **49**, 6280 (1994).
- [9] G. Hampel, B. Batlogg, K. Krishana, N.P. Ong, W. Prusseit, H. Kinder, A.C. Anderson. *Appl. Phys. Lett.*, **71**, 3904 (1997).
- [10] D.V. Shantsev, M.E. Gaevski, R.A. Suris, A.V. Bobyl, V.E. Gasumyants, O.L. Shalaev. *Phys. Rev. B*, **60**, 17 (1999).
- [11] D.A.J. Bruggeman. *Ann. Phys. (Leipzig)*, **24**, 636 (1935).
- [12] X.C. Zeng, D.J. Dregman, P.M. Hui, D. Stroud. *Phys. Rev. B*, **38** (15), 10 970 (1988).
- [13] К.К. Лихарев. *Введение в динамику джозефсоновских переходов* (М., Наука, 1985).
- [14] Л.Д. Ландау, Е.М. Лифшиц. *Электродинамика сплошных сред* (М., Наука, 1988).

Редактор Л.В. Беляков